Original Research Article

International journal of spray and combustion dynamics

International Journal of Spray and Combustion Dynamics
2016, Vol. 8(4) 262–270

DOI: 10.1177/1756827716641118
scd.sagepub.com

SAGE

Theoretical investigation of the particle response to an acoustic field

Javier Achury and Wolfgang Polifke

Abstract

In this paper, the problem of a particle subjected to an acoustic field is addressed theoretically. Once the fundamental equation of motion is obtained, two nonlinearities are identified: one related to the drag law and one associated with the excitation. In order to face the nonlinearities, two cases are constructed: the first corresponds to the parametric numerical solution of a particle with nonlinear drag in an oscillating flow field (infinite wavelength) and the second refers to the particle submitted to an acoustic standing wave (finite wavelength). For the latter, an approximated analytical solution is formulated. The system is linearized around an equilibrium point and the parameters of the equation are grouped in three nondimensional numbers: the Stokes number (S_t), the acoustic Mach number (M_a), and the densities ratio (γ). Conditions of parametric resonance in the particle response are deduced for this system by means of the analytical method here proposed, based on Hill's determinants. Comparison with numerical solutions of the linearized and nonlinearized equations close to an equilibrium point corroborates the analysis for different combinations of parameters.

Keywords

Particle response, Hill's determinant, parametric resonance

Date received: 2 December 2015; accepted: 29 February 2016

Introduction

The particle response to an acoustic field is a fundamental problem faced in the investigation of the multiple interactions that may occur in a polydispersed population of particles immersed in an acoustic field. This response is of primary interest in technologies that involve sprays, like spray combustion, or in devices that use forced fields to agglomerate particulate material (fine particles with sizes on the order of nanometers up to a few micrometers) in order to enhance filtration capacity.

In spray flames, for instance, number droplet density waves and droplet agglomeration are undesirable for a stable combustion process. Combustion instabilities appear when oscillations of heat release and pressure waves are in phase. While pressure oscillations are normally associated with the acoustic modes of the combustor, fluctuations in heat release can be generated by unsteady fuel evaporation or fluctuating equivalence ratios.[1] Under some conditions, acoustics promotes the formation of a number density wave of fuel droplets. In that case, a perturbed field of equivalence ratio, and subsequently of heat release, can be directly linked to acoustics.

In contrast, in some systems, agglomeration of particles due to acoustics is a beneficial phenomena and has a potential use in air pollution control.[2] Acoustic agglomeration is in this context a promising novel alternative to improve the particulate material filtration effectiveness in exhaust systems,[3,4] and, consequently, reduce the emissions of this product in diesel engines, just to mention one application.

Mechanisms of acoustic agglomeration or formation of a number density wave in a population of particles depend fundamentally on the individual particle dynamics (or response) to an acoustic field, which

Professur für Thermofluiddynamik, Technische Universität München, Germany

Corresponding author:
Javier Achury, Professur für Thermofluiddynamik, Technische Universität München, D-85747 Garching, Germany.
Email: achury@tfd.mw.tum.de

motivates the present investigation. Unfortunately, this dynamics is in general nonlinear, there are several parameters involved and the role of each parameter needs to be clearly understood in order to construct solid physical descriptions of the aforementioned mechanisms. It is pertinent to clarify that there are hydrodynamic mechanisms of acoustic agglomeration of binary nature.[5] These are activated by the interaction of two particles in a pressure field that is disturbed by the particles themselves. Such mechanisms require an explicit description of the disturbed field around the particles and is out of the scope of the analysis given here.

Although several experiments[2,6] and numerical simulations[3,7–9] for different scenarios of an individual particle and population of particles submitted to an acoustic field have been carried out, in our best knowledge, a theoretical approach of the problem of a particle immersed in an acoustic field considering nonlinearities and focused on the examination of the parameters role has not yet been performed, which is the main novelty of the present investigation. Partial approximations have been carried out, for example, Aboobaker et al.[10] developed an approximate analytical description for the trajectory of a particle subjected to an acoustic standing wave. An acoustic force was contemplated in such work, which is the time-averaged force due to the drag produced by the acoustic field in the Stokes regime. That approach differs from ours as we attempt both to develop solutions without averaging in time any term in the equation of motion and to focus on the most general parametric response, seeking a procedure to estimate the particle drift velocity when the response is stable and particular conditions that lead to unstable or resonant responses.

The derivation of the equation of motion for a particle excited with an acoustic field is given in the following section, where two sources of nonlinearities are found. Next, the effect of the first nonlinearity, concerning the drag law, is evaluated numerically considering an oscillating flow as the particle excitation. Subsequently, a linearized equation is derived from the nonlinear problem involving an acoustic standing wave, and a principal stability map is constructed assuming a particular solution in complex Fourier series. Finally, the principal stability map is validated comparing the numerical solution with the theoretical response for several combinations of parameters.

Single droplet dynamics

The starting point of the investigation can be formulated as made by Sujith et al.[11] The Lagrangian equation of motion of a rigid spherical particle (subscript p is related to a particle and c to the fluid around it), without internal circulation nor angular motion, with mass m_p and velocity u_p can be stated as

$$m_p \frac{du_p}{dt} = F_D + F_{uf} + F_b + F_{vm} + F_{Basset} \tag{1}$$

Body forces F_b, the virtual mass force F_{vm}, and the Basset or history integral force F_{Basset} are not considered in this investigation. The remaining forces acting on the particle are the steady-state drag F_D and the undisturbed flow forces F_{uf}. The latter is the force required to accelerate the fluid of volume V_p if the particle were absent,[12] and is divided in the contributions of the pressure gradient and shear stress, $F_{uf} = V_p(-\partial p/\partial x + \partial \tau/\partial x)$. Since the acoustic field will be imposed, the shear stress is assumed to be zero and the pressure gradient becomes $\partial p/\partial x = -\rho_c \partial u_c/\partial t$. This is advantageous since the undisturbed flow force can be explicitly expressed in terms of the excitation of the fluid velocity field u_c. F_{uf} does not contribute significantly for a particle in gas flows where the density ratio $\gamma = \rho_p/\rho_c$ is much larger than unity,[13] but it will be maintained to preserve the generality of the approach. The drag force

$$F_D = \frac{1}{2}\rho_c C_D A_p |u_c - u_p|(u_c - u_p) \tag{2}$$

depends on the drag coefficient, defined as $C_D = f_1 24/Re_p$. The particle Reynolds number is $Re_p = |u_c - u_p| D_p/\nu_c$, where D_p is the particle diameter and ν_c the fluid kinematic viscosity. A_p is the cross-sectional area of the spherical particle. The drag force contributes with a linear term to the equation of motion for the Stokes regime and with a nonlinear term for the Schiller and Naumann extension in the following way

$$f_1 = \begin{cases} 1 & \rightarrow \text{ Stokes flow. } Re_p < 1 \\ 1 + 0.15 Re_p^{0.687} & \rightarrow \text{ Schiller and Naumann. } Re_p < 800 \end{cases}$$

Assembling the terms, the following governing equation is obtained

$$\gamma \frac{\mathrm{d}u_r}{\mathrm{d}t} = -\frac{3C_D}{4D_p} u_r |u_r| - (\gamma - 1)\frac{\partial u_c}{\partial t} \tag{3}$$

where $u_r = u_p - u_c$. Given that $\ddot{x}_p = \dot{u}_p$ and $\dot{x}_p = u_p$, the equation of motion for $C = 18\nu_c/\gamma D_p^2$ can be expressed as

$$\ddot{x}_p + f_1 C \dot{x}_p = f_1 C u_c + \frac{1}{\gamma}\frac{\partial u_c}{\partial t} \tag{4}$$

Two nonlinearities contained in particular forms of f_1 and u_c are identified. The first one is associated with

the exponent in the particle Reynolds number for non-Stokes flow. The second one comes from the excitation u_c, which leads to two cases: oscillating flow (excitation with infinite wavelength and speed of sound) and acoustic (finite wavelength). For the latter, the velocity field depends on the particle position x_p ($u_c(x_p, t)$). These two nonlinearities will be faced numerically for f_1 and analytically for u_c, in the following sections. Note that only in the simplest case where $f_1 = 1$ (Stokes flow) and $u_c = \hat{u}_c \sin(\omega_f t)$ (oscillating flow) an analytical solution of equation (4) can be easily derived.

Particle in an oscillating flow field

In the present context, an oscillating flow field refers to an acoustic wave with infinite wavelength, which is equivalent to consider an incompressible medium or with infinite speed of sound. The flow velocity oscillates according to $u_c(t) = \hat{u}_c \sin(\omega_f t)$, where $\hat{u}_c$ is the amplitude of the velocity wave and $\omega_f = 2\pi f_r$ is the angular frequency. For this form of excitation, a nondimensional equation can be derived from equation (4). After defining the nondimensional time $\tau = \omega_f t$, the Stokes number $S_t = f_r/C$ and the nondimensional velocity $u_p^* = u_p/\hat{u}_c$, the governing equation becomes

$$\frac{\mathrm{d}u_p^*}{\mathrm{d}\tau} = -\frac{f_1}{2\pi S_t}\left(u_p^* - \sin(\tau)\right) + \frac{1}{\gamma}\cos(\tau) \qquad (5)$$

If the Schiller and Naumann extension for the drag law is accounted for ($f_1 = f_1(Re_p)$), equation (5) becomes nonlinear and is resolved numerically, following Sujith et al.[11] This initial value problem is resolved parametrically for a range of Stokes numbers using the Runge–Kutta algorithm. Different amplitudes of excitation $\hat{u}_c$ are also evaluated, which allows the assessment of corresponding maximum values of the Reynolds number ($Re_{p,max}$) in the particle response.

The entrainment factor, $\eta = \hat{u}_p/\hat{u}_c$, defined as the velocity amplitudes ratio (or the amplitude of u_p^*) is plotted in Figure 1 as a function of the Stokes number and the corresponding $Re_{p,max}$. The entrainment factor was determined as the amplitude of the discrete Fourier transform of the nondimensional particle velocity u_p^* at the frequency f_r. The response of the particle is strongly sensitive to the Stokes number, which relates, for this case, the characteristic time response of the particle $\tau_C = 1/C$ with the period of the flow oscillation. For high frequencies and large diameters (high Stokes numbers) the particle does not react fast enough and the entrainment factor η becomes weak. In the regime of Stokes flow (small Re_p), and consequently the limiting case where $f_1 = 1$, the differential equation (5) is linear and the entrainment factor

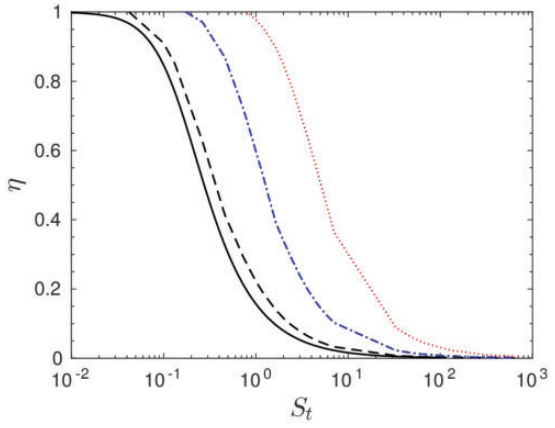

Figure 1. Entrainment factor (η) against Stokes number ($S_t = f_r/C$) and maximum particle Reynolds numbers. —- $Re_{p,max} < 1$, – – – $Re_{p,max} = 20$, – · – $Re_{p,max} = 100$, and · · · $Re_{p,max} = 1000$.

is associated uniquely to the Stokes number.[11] In fact, the nonlinear effect of increased drag at higher Re_p is to shift the entrainment factor curve to the right side of Figure 1. The Stokes flow assumption can be employed in the equation of motion (4) only for a combination of a low relative velocity u_r, small particle size D_p and a large fluid viscosity ν_c. Small relative velocities may be expected for small excitation amplitudes of u_c and a nonresonant particle velocity u_p.

Particle in an acoustic standing wave

The previous section corresponds to a limiting case where the acoustic wavelength λ is infinite. For finite wavelengths, the intensity of the standing wave depends on the position x_p, then

$$u_c(x_p, t) = 2\hat{u}_c \sin(\omega_f t)\cos\left(\frac{2\pi}{\lambda}x_p\right) \qquad (6)$$

The factor of 2 arises from the superposition of two travelling waves, each one with amplitude $\hat{u}_c$.

The, apparently simple, nonlinear dependence of excitation amplitude on particle position brings an interesting theoretical wealth to the problem. From equation (4), the following system for an acoustic standing wave is derived

$$\begin{aligned} \dot{u}_p &= -Cf_1\dot{x}_p + 2f_1 C\hat{u}_c \sin(\omega_f t)\cos\left(\frac{2\pi}{\lambda}x_p\right) \\ &\quad + 2\frac{\omega_f}{\gamma}\hat{u}_c \cos(\omega_f t)\cos\left(\frac{2\pi}{\lambda}x_p\right) \\ \dot{x}_p &= u_p \end{aligned} \qquad (7)$$

Besides being nonlinear, equation (7) depends on seven parameters: D_p, $\hat{u}_c$, λ, ω_f, ρ_c, ρ_p, and ν_c. Our goal is to investigate the parametric stability of system (7).

Theoretical approach for the nonlinear system

The purpose of nonlinear analysis is to detect a rich variety of phenomena introduced by the nonlinear terms, which is normally focused on the system behavior around the equilibrium points. Sub- or super harmonics resonances, parametric instabilities in pulsating loads, and existence of periodic solutions are typical phenomena associated with nonlinearities.[14] The canonical notation of the nonlinear, parametric, and nonautonomous (a differential equation where the coefficients depend explicitly on the independent variable, t in this case, is by definition nonautonomous) system is $\dot{\mathbf{x}} = f(\mathbf{x}, \mathbf{p}, t)$ ($\mathbf{p}$ is the vector of parameters). In an equilibrium point $(x_e, \mathbf{p})$, the vector $\dot{\mathbf{x}}$ vanishes, making $f(\mathbf{x}_e, \mathbf{p}, t) = 0$. By inspection of system (7), the equilibrium points are located at the standing wave nodes, $x_e = (2m+1)\lambda/4$. At the first equilibrium point $(x_e, u_e) = (\lambda/4, 0)$, the system is linearized by means of the Jacobian matrix

$$\begin{pmatrix} \dot{u}_p \\ \dot{x}_p \end{pmatrix} = \begin{pmatrix} -C & -\frac{4\pi\hat{u}_c C}{\lambda}\sin(\omega_f t) - \frac{4\pi\omega_f\hat{u}_c}{\lambda\gamma}\cos(\omega_f t) \\ 1 & 0 \end{pmatrix} \begin{pmatrix} u_p \\ x_p \end{pmatrix} \tag{8}$$

This system can be represented as $\dot{\mathbf{x}} = \mathbf{A}(t)\mathbf{x}$. In order to study the type of local stability, Floquet analysis, perturbation methods and harmonic balance were initially considered.

Brief discussion on the selected method

As matrix $\mathbf{A}(t)$ is periodic, the system is amenable to Floquet analysis. According to the Floquet theory in a periodic varying system, like system (8), there is a fundamental matrix solution $\boldsymbol{\Phi}(t)$ that can be decomposed as the product of a periodic matrix $\mathbf{P}(t)$ and an exponential matrix $e^{t\mathbf{B}}$, $\boldsymbol{\Phi}(t) = \mathbf{P}(t)e^{t\mathbf{B}}$. The stability of the solution is in general determined by matrix $\mathbf{B}$. Nevertheless, as mentioned by Montagnier,[15] Floquet theory is not easy to use for quantitative purposes, since there is no set procedure of determining the Floquet factors ($\mathbf{B}$ matrix), unless numerically by posing a boundary value problem, for specific values on the parameters. Additionally, the periodic matrix $\mathbf{P}(t)$, in case it can be determined, does not explicitly show the presence of harmonic or sub-harmonic frequencies in the response.

Although the parameters can be grouped into three, as will be shown later, multiple scales or perturbation methods tend to be complicated for even two parameters and not easily generalizable. In contrast, the Hill's determinants (based on a harmonic balance) technique is in principle not limited to a low number of parameters and allows to incorporate explicitly harmonics and sub-harmonics in the response. For these reasons this strategy is used here.

Making an analogy, system (8) can be seen as a damped harmonic oscillator with periodic spring coefficient

$$\ddot{x}_p + \underbrace{C}_{\text{damping}}\dot{x}_p + \underbrace{f(t)}_{\text{spring coeff.}}x_p = 0, \tag{9}$$

where

$$f(t) = \frac{4\pi\hat{u}_c C}{\lambda}\sin(\omega_f t) + \frac{1}{\gamma}\frac{4\pi\hat{u}_c\omega_f}{\lambda}\cos(\omega_f t) \tag{10}$$

The time varying "spring coefficient" can cause a particular type of resonance called *parametric resonance*. In a linear system, parametric resonance could be understood as how the oscillatory response grows due to the periodic variation of some energy-storing parameter,[16] and is essentially different from resonance that may occur in an oscillator of constant parameters with external forcing. Compared to the classic resonance, there are two main peculiarities of parametric resonance in a linear system (like equation (9)): first, there is a different relationship between the mean natural frequency of the system and the frequency of the parameter modulation ω_f, and second, if damping or friction exists, parametric resonance occurs only above a threshold in the amplitude of the parameter modulation $f(t)$.[17] Details of these two facts will be discussed later when an assumed solution needs to be constructed. In this work, a transformation $q(t) = x_p(t)e^{\frac{C}{2}t}$ is applied, which eliminates explicitly the term related to damping. Equation (9) now reads

$$\ddot{q}(t) + \left(-\frac{C^2}{4} + f(t)\right)q(t) = 0 \tag{11}$$

A Hill's equation[18] is therefore obtained. Note that one particular case of the Hill's equation is the Mathieu equation, where $f(t) = \beta\cos(t)$. Methods to find approximate solutions and construct stability maps for the Mathieu equation have been extensively applied,[14,18,19] and served partially as inspiration for the procedure developed here. Invoking the nondimensional time $\tau = \omega_f t$, the particular form for the Hill's equation of our problem can be conveniently expressed as

$$\ddot{q}(\tau) + \left(-\left(\frac{1}{4\pi S_t}\right)^2 + \frac{M_a}{\pi S_t}\sin(\tau) + \frac{2M_a}{\gamma}\cos(\tau)\right)q(\tau) = 0 \tag{12}$$

Three dimensionless numbers are identified: S_t, γ and M_a. The Stokes number S_t and the densities ratio γ were introduced in the previous two sections. The nondimensional number $M_a = 2\pi\hat{u}_c/\lambda\omega_f$ is in fact an acoustic Mach number ($M_a = \hat{u}_c/\bar{c}$, where the speed of sound is $\bar{c} = \lambda f_r$). An alternative interpretation of this number is the acoustic displacement $\hat{u}_c/f_r\lambda$, which is the ratio of the oscillation displacement ($\hat{u}_c/f_r$) and wavelength (λ).

Presumed solution

Initially, periodic solutions are sought, thus, a complex Fourier series is assumed to satisfy equation (12)

$$q(\tau) = \sum_{n=-\infty}^{n=+\infty} c_n e^{in\tau} \tag{13}$$

Taking the second derivative for the series, the Euler formula for sinus and cosinus and replacing them into equation (12), results in

$$-\sum_{n=-\infty}^{n=+\infty} n^2 c_n e^{in\tau} - \left(\frac{1}{4\pi S_t}\right)^2 \sum_{n=-\infty}^{n=+\infty} c_n e^{in\tau} + \left(\frac{M_a}{\pi S_t}\left(\frac{e^{i\tau} - e^{-i\tau}}{2i}\right) + \frac{2M_a}{\gamma}\left(\frac{e^{i\tau} + e^{-i\tau}}{2}\right)\right) \sum_{n=-\infty}^{n=+\infty} c_n e^{in\tau} = 0 \tag{14}$$

Developing the product, grouping the exponents and performing a change of indexes, the following is obtained

$$\sum_{n=-\infty}^{n=+\infty} c_n e^{in\tau}\left(n^2 + \left(\frac{1}{4\pi S_t}\right)^2\right) + \sum_{n=-\infty}^{n=+\infty} c_{n+1} e^{in\tau}\left(\frac{iM_a}{2\pi S_t} - \frac{M_a}{\gamma}\right) + \sum_{n=-\infty}^{n=+\infty} c_{n-1} e^{in\tau}\left(-\frac{iM_a}{2\pi S_t} - \frac{M_a}{\gamma}\right) = 0 \tag{15}$$

Then, the series can be factorized and a recursive relation for the coefficients c_n is derived

$$\left(-\frac{iM_a}{2\pi S_t} - \frac{M_a}{\gamma}\right)c_{n-1} + \left(n^2 + \left(\frac{1}{4\pi S_t}\right)^2\right)c_n + \left(\frac{iM_a}{2\pi S_t} - \frac{M_a}{\gamma}\right)c_{n+1} = 0 \tag{16}$$

Equation (12) has a nontrivial solution in form of a complex Fourier series (13) only if the coefficients c_n are all not zero. This condition is guaranteed if the determinant of the linear system that results from the collection of the recursive relations to find the coefficients c_n is zero ($\det(H_N) = 0$). A finite limit to the series N can be taken based on the property of convergence of the Hill's determinant,[18] which yields for the present case

$$\det(H_N) = \begin{vmatrix} N^2 + \left(\frac{1}{4\pi S_t}\right)^2 & \frac{iM_a}{2\pi S_t} - \frac{M_a}{\gamma} & 0 & 0 & 0 & 0 & 0 \\ -\frac{iM_a}{2\pi S_t} - \frac{M_a}{\gamma} & \cdots & \cdots & 0 & 0 & 0 & 0 \\ 0 & \cdots & \cdots & \cdots & 0 & 0 & 0 \\ 0 & 0 & \cdots & \cdots & \cdots & 0 & 0 \\ 0 & 0 & 0 & \cdots & \cdots & \cdots & 0 \\ 0 & 0 & 0 & 0 & \cdots & \cdots & \frac{iM_a}{2\pi S_t} - \frac{M_a}{\gamma} \\ 0 & 0 & 0 & 0 & 0 & -\frac{iM_a}{2\pi S_t} - \frac{M_a}{\gamma} & N^2 + \left(\frac{1}{4\pi S_t}\right)^2 \end{vmatrix}$$

If $\det(H_N) = 0$ is resolved an algebraic equation is obtained. Although this algebraic equation is implicit (it can not be expressed explicitly for any contained parameter), it can be eventually factorized producing different branches (roots of the implicit equation) in its solution. The number of branches is equal to the limit of the series N. In Figure 2, such implicit equation is plotted for $N = 18$, $N = 22$, and $N = 26$ as function of the parameters S_t and M_a, for $\gamma = 816$. Setting a large limit (N) for the series ensures the convergence of the branches close to the $M_a = 0$ axes.

The solid lines in Figure 2, which have a tongue shape, can be interpreted as combinations of parameters that produce a periodic solution for $q(t)$ composed by a combination of N harmonics. As the solution for these tongues are periodic, this would suggest that in the points that do not belong to these lines some decay/growth rate in the response could be expected. In order to extend the analysis for these points, the assumed

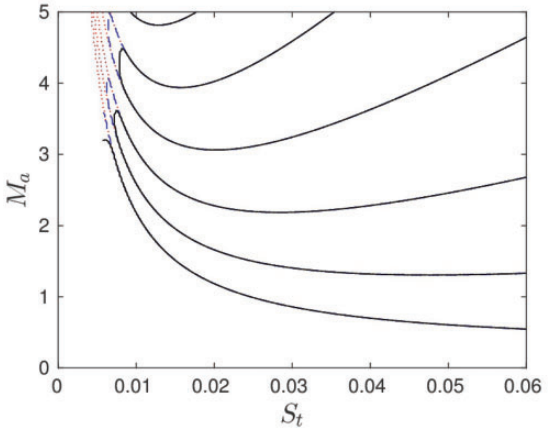

Figure 2. Roots of the implicit equation derived from the Hill's determinant and its convergence as the series limit N is augmented ($\cdots$ $N = 18$, – – $N = 22$, —- $N = 26$). Continuous lines indicate the combination of parameters that lead to periodic solutions for $q(t)$ (equation (12)) composed by the combination of N harmonics ($\gamma = 816$).

solution needs to be modified in order to include a real growth/decay rate ω_n, and, since there are no additional equations available, it needs to be decided which harmonic is dominant. Additionally, as in the parametric equation (9) a sub-harmonic response could be involved, is also incorporated in the presumed solution, making it more general. This yields

$$q(\tau) = \sum_{n=-\infty}^{n=+\infty} c_n e^{\left(\frac{\omega_n}{\omega_f}+\frac{in}{2}\right)\tau} \tag{17}$$

Since $x_p(t) = q(t)e^{-\frac{C}{2}t}$, an unstable response will be reached for $x_p(t)$ if $q(t)$ grows faster than $e^{\frac{C}{2}t}$, which determines a critical grow rate of $C/2$ that produces periodic solutions in $x_p(t)$. These exponential and periodic contributions can be seen more clearly in terms of the particle trajectory equation

$$x_p(\tau) = \sum_{n=-\infty}^{n=+\infty} c_n \underbrace{e^{(\omega_n - C/2)\frac{\tau}{\omega_f}}}_{\text{exponential}} \underbrace{e^{in\tau}}_{\text{periodic}} \tag{18}$$

A stable particle response occurs if the grow rate is negative ($\omega_n - C/2 < 0$), which implies that the particle will be attracted to the closest velocity node. In contrast, an unstable response occurs for a positive grow rate ($\omega_n - C/2 > 0$), where the particle oscillation grows indefinitely.

Developing the same procedure outlined before, the corresponding recursive relation for the response in terms of sub-harmonics with grow/decay rate (equation (17)) is

$$\left(-\frac{iM_a}{2\pi S_t} - \frac{M_a}{\gamma}\right)c_{n-2} + \left(-\left(\frac{\omega_n}{\omega_f} + i\frac{n}{2}\right)^2 + \left(\frac{1}{4\pi S_t}\right)^2\right)c_n + \left(\frac{iM_a}{2\pi S_t} - \frac{M_a}{\gamma}\right)c_{n+2} = 0 \tag{19}$$

As a total of N growth/decay rates ω_n were introduced, an additional assumption needs to be made. Let us consider that only the first sub-harmonic has a critical growth rate $\omega_1 = C/2$ (then $\omega_1/\omega_f = 1/4\pi S_t$), while $\omega_n = 0$ for $n \neq 1$. The stability map derived from this recursive relation is plotted in Figure 3, where two unstable regions with a growth rate in the first sub-harmonic satisfy equation (9). It predicts the nature of the response of the linearized equation (9) for any combination of the parameters S_t and M_a ($\gamma = 816$).

Limits of physical validity

The calculated isolines for the maximum Re_p and the relative Mach number $M_r = |u_p - u_c|/\bar{c}$ (assuming Stokes flow in the governing equation) obtained for the particle oscillatory motion help to establish the limits of physical validity of the approach. Some of these lines are plotted in Figure 3 (right). For the stable region, the zones of Stokes and non-Stokes flow are limited by the isoline $Re_p = 1$. It can be appreciated in Figure 3 (right) that there is an important regime of nonlinear drag in the stable region ($Re_p > 1$). The limit of nonlinear drag for the Schiller and Naumman extension $Re_p \approx 800$ is even beyond the interval shown in Figure 3.

For low particle Reynolds numbers, the drag coefficient C_D uniformly decreases as the relative Mach number M_r increases.[13] This dependence, $C_D(M_r)$, not accounted for in the governing equation, can be neglected in most of the stable region, given that the values of the isolines of M_r are relatively small. However, in a resonant response (unstable region) the relative Mach number can be large and C_D will diminish accordingly,

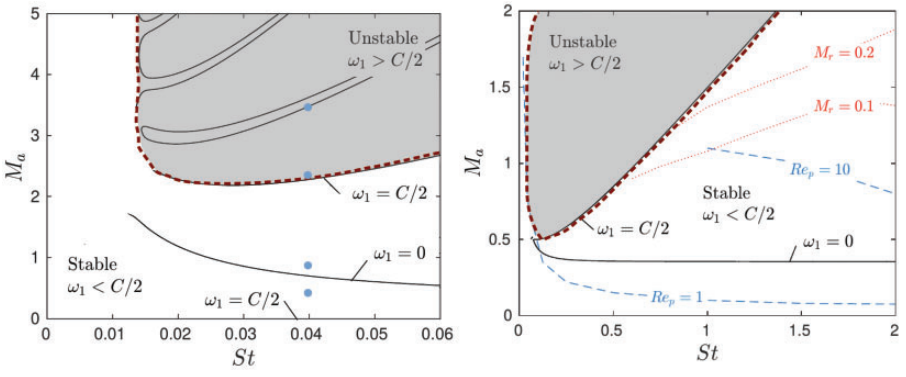

Figure 3. Principal stability map for equation (9) for the intervals $0 \leq St \leq 0.06$ (left) and $0 \leq St \leq 2$ (right). The two filled regions indicate that the particle response has a growth rate and are unstable. Note that the filled tongue of the left figure is not visible on the right one. The unstable and stable regions are divided by the dashed line that determines if the response is resonant or not ($N = 25$ and $\gamma = 816$).

introducing a different dynamics on the particle than predicted by the stability map. This reduction in the drag is due to the rarefied flow, in which the thickness of the shock wave and related drag wave is comparable to the particle size.[13] Instead of creating a shock wave on the particle, in the rarefied flow, the particle is engulfed by the shock wave. The dependence of C_D on M_r cannot be overlooked for unstable regions. However, it does not affect severely either the predicted responses in the stable region or the inception of unstable responses determined by the line that separates stable from unstable regions.

It can be argued that, in practice, high values of M_a would be difficult to obtain since high acoustic standing wave amplitudes were required, which, in addition, cannot be described with linear acoustics theory. In fact, for large acoustic pressure amplitudes, one of the nonlinear effects is the harmonic standing waveform distortion due to the shock wave development.[20] The sinusoidal waveform turns into an N shape for high amplitude acoustic pressures in an effect known as acoustic saturation. In this sense, it could be pointed out that means to generate high amplitude acoustic standing waves preventing shock waves have been proposed. This can be reached with shape optimization of the cavity where the standing wave is produced, or by the use of multiple Helmholtz resonators. Acoustic pressures obtained with the former method can reach four times the ambient pressure.[21] Therefore, the potential model limitation of assuming a sinusoidal waveform in the excitation can be suppressed, at least technically, even for high amplitude (or nonlinear) acoustics.

Particle drift velocity

The particle drift velocity, i.e. the velocity at which the particle approaches to the node in each oscillation, can be estimated by means of the predicted decay rate ω_1 in the stable region. In fact, the exponential part of equation (18) evolves the oscillatory trajectory of the particle to the equilibrium point. For $M_a = 0$ (infinite wavelength), the decay rate is $\omega_1 = C/2$ and there is no drift velocity. Since there are no nodes the particle oscillates with a calculable entrainment factor (see section ''Particle in an oscillating flow field''). As M_a grows from zero, in the stable region, the decay rate decreases from $\omega_1 = C/2$ to the line where $\omega_1 = 0$ indicated in Figure (3). In this zone, the response is dominated by the first harmonic as the decay rate for the first sub-harmonic is smaller. Above the line where $\omega_1 = 0$, the first sub-harmonic becomes dominant, because its decay rate is larger than the decay rate of the first harmonic. The first sub-harmonic decay rate grows continuously until it reaches the line of resonant response $\omega_1 = C/2$ (dashed line in Figure 3).

The importance of sub-harmonics

The need to develop solutions in terms of sub-harmonics is not arbitrary. It is derived from the fact that parametric resonance occurs when the frequency of parameter modulation is twice the natural frequency oscillation of the system.[16] In a resonant condition, when the amplitude of the source $f(t)$ provides energy to the system in such a way that exceeds the energy dissipated by the damping term C (see equation (9)), the net work done by the modulated ''spring'' force, $F(t) = f(t)x_p(t)$, during one period of oscillation is equal to the change of energy of oscillation in the same period. If the differential work done by the force $F(t)$ is $\mathrm{d}W = -F(t)\mathrm{d}x_p$ and $\mathrm{d}x_p = u_p\mathrm{d}t$, the work done in a period of oscillation is

$$W = -\int_0^T f(t)x_p(t)u_p(t)\mathrm{d}t \tag{20}$$

The maximal work is given when the principal frequency of the response $x_p(t)$ (or $u_p(t)$) is half of the parameter modulation frequency, $\omega_f/2$. In this condition there is a maximal energy transfer from the modulated parameter to the system,[17] although energy transfer is also possible, with less intensity, at different frequencies.

Verification of the theoretical model

The nature of the particle response is corroborated numerically by resolving both the original nonlinear and the linearized systems, equations (7) and (8), respectively, close to the first equilibrium point $x_p = \lambda/4$. In both cases the same numerical Runge–Kutta algorithm and initial conditions ($x_p = 1.02\lambda/4$, $\dot{x}_p = 0$) were employed. A particular Stokes number of $S_t = 0.04$ and several values of M_a were taken, as illustrated with dots in Figure 3 (left). As expected, there is an impressive variety of solutions dominated by the first harmonic and sub-harmonic in stable, periodic and unstable forms.

The particle response for the parameters $M_a = 0.5$, $M_a = 1$, and $M_a = 2.4$ are plotted in Figure 4. The responses for $M_a = 0.5$ and $M_a = 1$ belong to a stable region where the particle approaches always to the nearest velocity node. Both responses, the nonlinearized and linearized, are identical as the solution is not resonant and initially close to the point of linearization. The solution for $M_a = 0.5$ is far from the influence of the sub-harmonic critical growth rate, therefore, the response is dominated by the first harmonic. The solution for $M_a = 1$ is closer to a line in the stability map (Figure 3) for a periodic sub-harmonic solution, but still in the stable region. Thus, this response is dictated by this mode decaying as shown in Figure 4. The

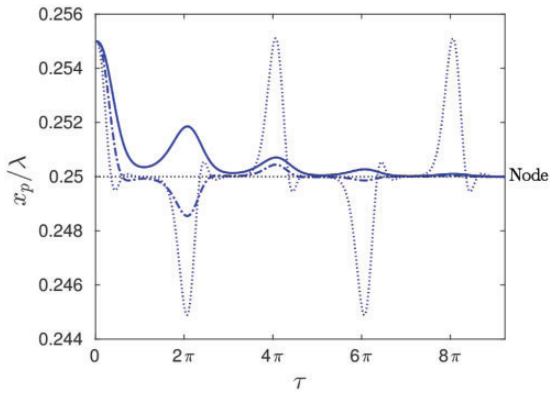

Figure 4. Numerical solutions of equations (7) and (8) (linearized and nonlinearized solutions are identical) close to the first equilibrium point (or velocity node), with initial conditions $u_p(0) = 0$, $x_p(0)/\lambda = 1.02/4$. $S_t = 0.04$, for —- $M_a = 0.5$, – · – $M_a = 1$ and · · · $M_a = 2.4$ ($\gamma = 816$).

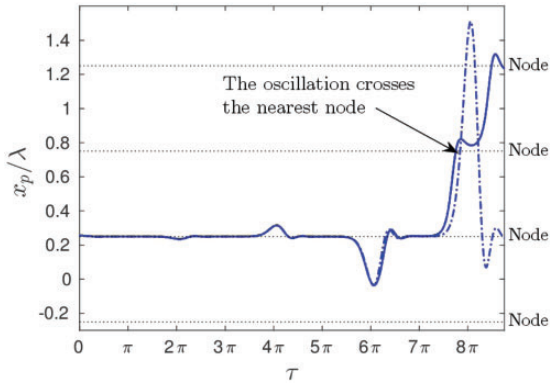

Figure 5. —- Numerical solution of the nonlinear system (equation (7)) and – · – Numerical solution of the linearized system (equation (8)). The initial particle position, $x_p(0)/\lambda = 0.255$, is close to one node but the response is resonant. $St = 0.04$, $M_a = 3.5$, and $\gamma = 816$.

solution for $M_a = 2.4$ falls in the line of Figure 3 that predicts a periodic solution dominated by the first sub-harmonic and this nature of the response is evidenced with the dotted line in Figure 4. Additionally, this periodic solution is not traced by a sinusoidal function, which legitimizes the need to describe the particle response by the interaction of several sub-harmonics and use a Fourier series for this effect in the presumed solution.

From $M_a > 2.4$ ($S_t = 0.04$) the response is resonant, as predicted by the first branch of the unstable region denoted in Figure 3 (left). The virtual line that separates the stable and unstable regions in the map is called here line of parametric resonance (dashed line in Figure 3).

As long as the particle trajectory moves away from the point of linearization (velocity node), as shown in Figure 5, for $M_a = 3.5$, the nonlinearized solution behaves differently than the linearized solution. The latter, in fact, predicts an exponential growth of the oscillation amplitude. As the nonlinear resonant oscillation approaches a neighbor node (equilibrium point), as appreciated in Figure 5, the nonlinear effect becomes evident. This nonlinear effect, denominated as *parametric regeneration*, restricts the resonant growth of the oscillation.[17] The velocity nodes act as particle attractors that establish the regenerated particle trajectories.

Conclusions

In this work, two nonlinearities present in the particle response to an acoustic field have been faced attempting a maximum generalization of the response based on its parameters. A theoretical approach for the solution of the nonlinear equation of motion for the particle in an acoustic standing wave close to an equilibrium point has been presented. For this case, a remarkable variety of stable and parametric resonant responses have been predicted theoretically and corroborated numerically. The dependence of the response, and consequently its stability, has been reduced from seven parameters to only three: the Stokes number S_t, the acoustic Mach number M_a, and the densities ratio γ. Thus, a proper generalization of the particle response has been reached. A stability map for the first sub-harmonic has been constructed for this reduced amount of non-dimensional numbers, which predicts the nature of the particle trajectories for any combination of parameters under the discussed limits of validity. The characteristics of the resonant response and the particle drift velocity for a nonresonant response were also outlined. Future work contemplates the need to include the drag coefficient dependence on large Mach numbers in order to extend the validity of the stability map.

Acknowledgements

We want to thank Dr Camilo Silva for his valuable support during the development of this investigation.

Declaration of conflicting interests

The author(s) declared no potential conflicts of interest with respect to the research, authorship, and/or publication of this article.

Funding

The author(s) disclosed receipt of the following financial support for the research, authorship, and/or publication of this article: This work was financially supported by a grant from the Colombian Administrative Department of Science, Technology and Innovation (Colciencias).

References

1. Candel S. *Combustion dynamics and control: Progress and challenges*. New York: Elsevier Inc., 2002, pp.1–28.
2. Robert E, Jajarmi R and Engvall K. Acoustic separation of sub-micron particles in gases. In: *Proceedings of meetings on acoustics*, vol. 19, Montreal, Canada, 2–7 June 2013.
3. Katoshevski D, Ruzal M, Shakked T, et al. Particle grouping, a new method for reducing emission of submicron particles from diesel engines. *Fuel* 2010; 89: 2411–2416.
4. Sun D, Zhang X and Fang L. Coupling effects of gas jet and acoustic waves on inhalable particle agglomeration. *J Aerosol Sci* 2013; 66: 12–23.
5. Gonzalez I, Gallego-Juarez J and Riera E. The influence of entrainment on acoustically induced interactions between aerosol particles - an experimental study. *J Aerosol Sci* 2003; 34: 1611–1631.
6. Jeong J and Woo J. Generation of a 25-MHz high-frequency ultrasound beam for acoustic particle trapping. *J Korean Phys Soc* 2013; 62: 238–242.
7. Markauskas D, Kacianauskas A and Maknickas A. Numerical particle-based analysis of the effects responsible for acoustic particle agglomeration. *Adv Powder Technol* 2015; 26: 698–704.
8. Markauskas D, Maknickas A and Kacianauskas R. Simulation of acoustic particle agglomeration in poly-dispersed aerosols. *Procedia Eng* 2015; 102: 1218–1225.
9. Kumara Gurubaran R and Sujith RI. An experimental investigation of non-evaporative sprays in axial acoustic fields. In: *46th AIAA - Aerospace sciences meeting and exhibit*, Reno, Nevada, 7–10 January 2008, AIAA 2008-1046.
10. Aboobaker N, Blackmore D and Meegoda J. Mathematical modeling of the movement of suspended particles to acoustic and flow fields. *Appl Math Model* 2005; 29: 515–532.
11. Sujith R, Waldherr G, Jagoda J, et al. A theoretical investigation of the behavior of droplets in axial acoustic fields. *J Vib Acoust* 1999; 121: 286–294.
12. Clift R, Grace JR and Weber ME. *Bubbles, drops and particles*. New York: Dover Publications, Inc., 1978.
13. Crowe T, Schwarzkopf S, Sommerfeld M, et al. *Multiphase flows with droplets and particles*. Boca Raton, FL: CRC Press, 2011.
14. Nayfeh A and Mook D. *Nonlinear oscillations*. New York: John Wiley and Sons, 2004.
15. Montagnier P, Spiteri R and Angeles J. The control of linear time-periodic systems using Floquet-Lyanupov theory. *Int J Control* 2004; 77: 472–490.
16. Butikov E. Parametric resonance. *Comput Sci Eng* 1999; 1: 76–83.
17. Butikov E. Parametric excitation of a linear oscillator. *Eur J Phys* 2004; 25: 535.
18. Jordan DW and Smith P. *Nonlinear ordinary differential equations*. Oxford: Oxford University Press, 2007.
19. Simakhina SV. *Stability analysis of Hill's equation*. Master's Thesis, University of Illinois, USA, 2003.
20. Soltes M. *Description and generation of large-amplitude acoustic fields in closed spaces*. PhD Thesis, Czech Technical University, Prague, 2015.
21. Li X, Finkbeiner J, Raman G, et al. Nonlinear resonant oscillations of a gas in optimized acoustical resonators and the effect of central blockage. In: *41st AIAA - Aerospace sciences meeting and exhibit*, Reno, Nevada, 6–9 January 2003, AIAA 2003-368.